Aust. J. Phys., 1995, **48**, 187–205

Recent Progress in High Field Magnetism*

Muneyuki Date†

Advanced Science Research Centre, Japan Atomic Energy Research Institute, Tokai, Naka-gun, Ibaraki 319–11, Japan.

Abstract

Recent progress in high field magnetism performed mainly in the Research Centre for Extreme Materials, Osaka University, is reported, with a short survey of the Centre's history. The main activities are in the fields of magnetism and superconductivity where a common keyword is highly correlated electron physics. A rich variety of effects such as metamagnetism, field-induced electronic transitions etc. is summarised. High field studies are also effective in the fields of atomic and molecular sciences; for example, field-induced transparency in liquid oxygen, and diamagnetic orientation of organic and biological materials. New frontiers in high field technologies are discussed, including a highly sensitive magnetometer using the dynamical Faraday effect.

1. Introduction—History of High Magnetic Field Generation

There has been growing interest in the application of high magnetic fields to study magnetic properties of various materials, mainly because the field can produce intrinsic change not only in magnetic materials but also in chemical and biological products. Today we can produce more than 30 Tesla (T) of DC field, more than 70 T with pulsed fields, and about 500 T is available if destructive magnets are used.

The history of generating high magnetic fields began with their discovery by Oersted in 1820 who found the first 'artificial field' induced by an electrical current. The second step was to concentrate magnetic flux using ferromagnetic materials as done by Faraday and others. This method was improved by Ewing and Low (1889), leading to a maximum field of 3·5 T and ferromagnetic saturation. The conventional electromagnet at the end of the 19th century could supply fields of up to 1 T.

Innovative progress was achieved by Kapitza (1924) who made a pulsed magnetic field up to 35 T by transforming the mechanical energy of a motor generator into magnetic energy. The DC field, on the other hand, was improved by Bitter (1939) using a water-cooled Bitter coil, which produced fields of 20 T. This field is now produced by superconducting magnets which have been used

* Refereed paper based on a plenary lecture given to the joint Sixth Asia Pacific Physics Conference and Eleventh Australian Institute of Physics Congress held at Griffith University, Brisbane, July 1994.

† Emeritus Professor of Osaka University, Japan.

0004-9506/95/020187$10.00

worldwide since around 1960. The maximum DC field has been obtained by a hybrid magnet consisting of a Bitter and superconducting magnet, leading to a net field of the order of 30 T.

During the Second World War, a new idea for generating strong magnetic fields was developed by compressing magnetic flux with an implosion technique using gun-powder Fowler *et al.* (1960). A similar compression technique was also invented by Cnare (1966) using an electromagnetic force. The method has been developed at the Institute for Solid State Physics (ISSP), University of Tokyo, by the Miura Group (Miura *et al.* 1992). Both methods can produce about 500 T in several microseconds, accompanied by the destruction of the coil system. So they are not adequate for precise measurements.

In 1970, the present author developed a new system which, in theory, can be used to produce an infinite non-destructive magnetic field using specially designed multi-layer coils (Date 1975). The practical design and construction of the new multi-layer magnet was carried out at Osaka University. Such magnets have been used by many researchers, both domestic and international, and more than 300 papers in the fields of condensed matter physics, chemistry, and biology, have been published since 1975. A short review of the magnet is given in the next section, while more details can be found in Date (1976) and Yamagishi and Date (1989).

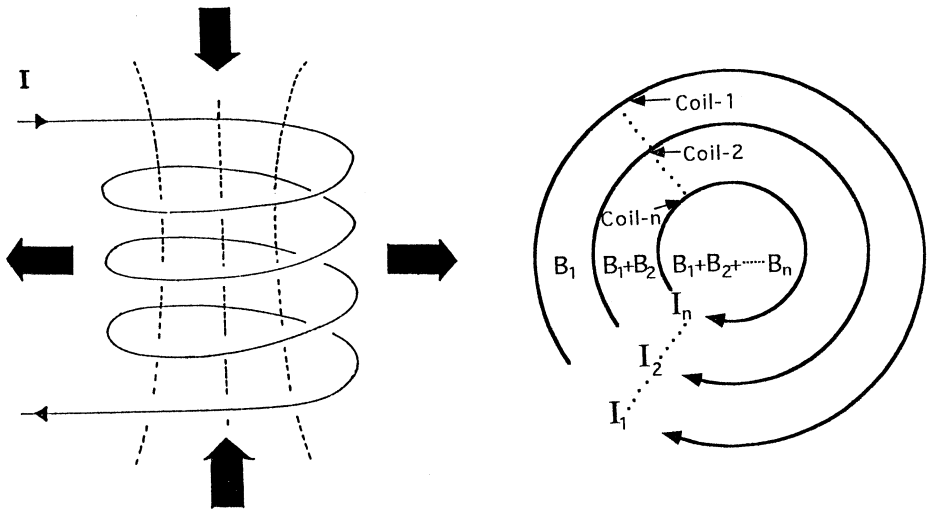

Fig. 1. Force acting on a coil (left) and schematic model of the multi-layer magnet (right).

2. Osaka Magnet—Multi-layer Coil System

It is impossible to produce an infinitely strong magnetic field in a single coil without destroying the system because of the strong electromagnetic force acting on the magnet. Kapitza was well aware of this difficulty, and concluded that the highest possible field was around 50 T even if the strongest material, for example steel, was used. We call this the Kapitza limit. As shown in Fig. 1 on the left, the force is axially compressible while it is explosive along the radial direction. The force is about 400 $\mathrm{kg\,mm^{-2}}$ at 100 T which is about four times larger than the tensile strength of normal steel.

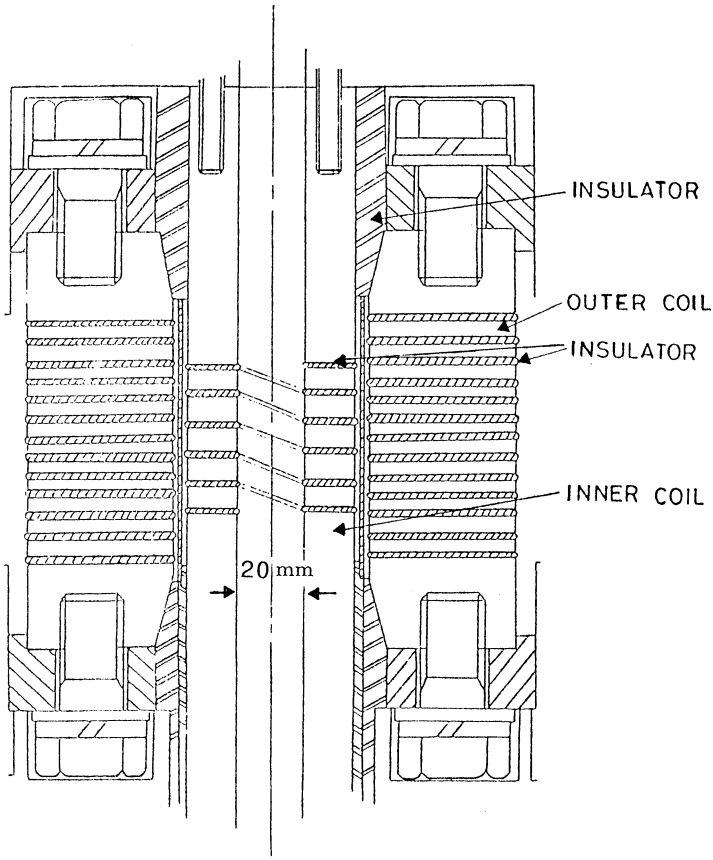

Fig. 2. Cross section of the standard two-layer magnet.

During the period 1970–75, the author developed a newly designed multi-layer coil system based on the idea that one can produce an infinitely strong magnetic field without destroying the coil if specially constructed multi-layer coils are used. The central idea is illustrated to the right of Fig. 1, where each circle means an independent magnet coil. The coil 1 produces the field B_1 by a current I_1; B_1 may be around 50 T within the Kapitza limit. The second coil 2 inside coil-1 produces the field B_2, but B_2 should be smaller than B_1 because the electromagnetic force acting in the coil 2 is proportional to B_1+B_2. Numerical calculation shows that $B_2 = 0{\cdot}62B_1$ for the safety limit of coil 2. Similarly, coils 3 to n are designed so that the expected resultant field B_r in coil n follows the relation

$$B_r > B_1\left(1 + \tfrac{1}{2} + \cdots + \frac{1}{n}\right). \tag{1}$$

This means that B_r goes to infinity for an infinite set of multi-layers. We have constructed various sets of the multi-layer magnet, and a test magnet with $n = 4$ produced a maximum field of 107 T in 2 mm diameter. The practical magnet now widely used is the two-layer magnet with a 2 cm inner diameter, as shown

explained in Fig. 5. The angular coupling of L and S in the $J = 2$ state, given in Fig. 5*a*, shows the presence of a transverse component of the spin which is not found in the $J = 1$ and 3 states. The exchange energy proportional to the transverse component should be taken into account for the c-plane. The analysis was done by the present author (Date 1989*b*) and the result is shown in Fig. 5*b*. The multistep magnetisation with moments $\frac{1}{3}$, $\frac{1}{2}$, $\frac{2}{3}$, $\cdots$ is found as expected from the theory and the agreement between theory (thin line) and experiment (thick line) is surprisingly good. The various fractional states appear because of constraints on the spin in the mixed states of the ground ($J = 1$) and excited ($J = 2$) spin chains.

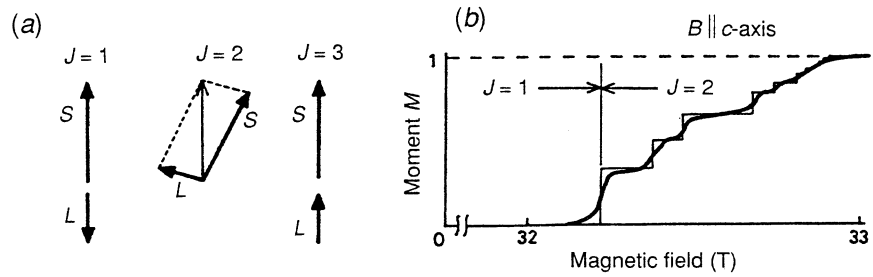

Fig. 5. (*a*) Vector model of the Fe spin in $CsFeCl_3$ and (*b*) the multistep magnetisation due to the $J = 1 \rightarrow J = 2$ crossover.

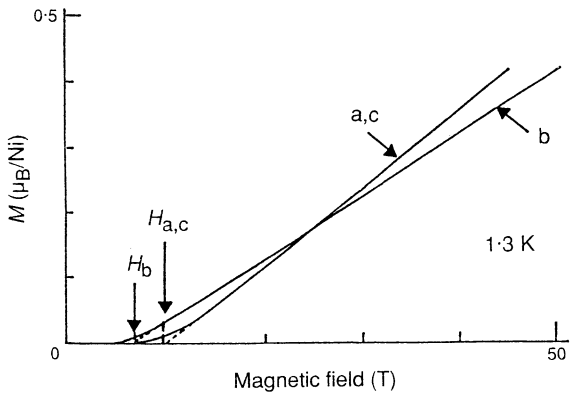

Fig. 6. Quenching of the non-magnetic Haldane state in NENP. Linear magnetisation appears above the critical fields H_a, H_b and H_c showing normal antiferromagnetism.

(4b) Quenching of the Haldane State under a High Field

There has been increasing interest in the energy gap in the linear chain Heisenberg antiferromagnet with spin $S = 1$, ever since Haldane conjectured that a chain of integer spins has an energy gap above the ground state. A high

field magnetisation study of NENP up to 50 T, one of the best materials to show the Haldane state, has been performed (Katsumata *et al.* 1989), as shown in Fig. 6 which reveals a field-induced quenching of the gap in NENP. The quenching is characterised by the critical field above which the system is in its usual antiferromagnetic state. Electron spin resonance of this material in high fields has been done our group (Data and Kindo 1990), and the anisotropy parameters of the first excited state investigated. A striking fact is that the sign of the anisotropy constant D in the ground state of Ni^{2+} is positive while that of the excited state triplet is negative. The result is explained by introducing a model where the excited state is the two-spin bound state with the resultant spin $S = 1$ moving in the chain like a soliton. The ESR data were analysed using the theory of spin-cluster resonance (Date and Motokawa 1966), leading to satisfactory agreement between theory and experiment.

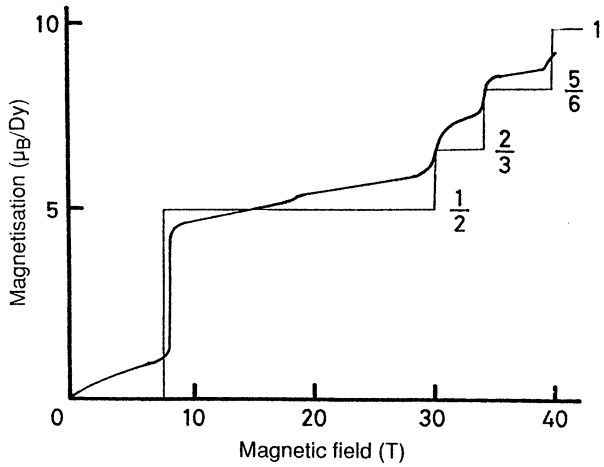

Fig. 7. Multistep magnetisation of DyAg along the ⟨111⟩ axis at $T = 4{\cdot}2$ K.

(4c) Quenching of the Quadrupole Order in DyAg

A multistep magnetisation observed in DyAg presents a new concept for high field magnetism. An example of the data is shown in Fig. 7 where the stepwise behaviour with the magnitudes of $\frac{1}{2}$, $\frac{2}{3}$, $\frac{5}{6}$ and 1 is illustrated. The thick curve shows the experimental results, while the thin lines show the theoretical step predictions, given by the following model. DyAg is a CsCl-type crystal with an antiferromagnetic transition at $T_N = 55$ K. Spins are parallel to four ⟨111⟩ directions with the four-sublattice model (Morin *et al.* 1989). A large quadrupole energy stabilises the spin structure. The observed step magnetisation is explained by keeping the quadrupole energy on each Dy site constant, while assuming that there is a quadrupole coupling energy between neighbouring Dy spins of the form $\frac{1}{2}(3\cos^2\theta_{ij}-1)Q_{ij}$, where Q_{ij} is the quadrupole coupling constant between i and j spins and θ_{ij} is the angle between spins. The total energy is calculated as the sum of the exchange, quadrupole and Zeeman energies and the standard mean field model. The experimentally obtained steps are explained by a simple spin-flop at the 0–$\frac{1}{2}$ transition and the successive three transitions are given by spin-flops with the rearrangement of the quadrupole order. Agreement between

theory and experiment is satisfactory as illustrated in Fig. 7. Three exchange parameters and three quadrupole coupling constants have been determined by this method (Yamagishi *et al.* 1990). Thus, DyAg is a typical example of the quenching of the quadrupole order under a high magnetic field.

(4d) Multistep Magnetisation in CeP

Recently, high quality single crystals of CeP were investigated using materials with a residual resistance ratio of 50 and the Schubnikov–de Haas oscillations. An unusual metamagnetism has been observed as shown in Fig. 8 (Kuroda *et al.* 1993). The metamagnetic transition fields are almost temperature independent from 1·3 to 35 K and lie with equal spacing on the H^{-1} scale. This result is explained in terms of the Stoner–Landau model. Namely, the magnetic transition of localised Ce spin is related to the Landau level crossing of up and down spin bands which split with the Stoner gap. The angular dependence of the multisteps is also investigated and a simple cubic symmetry with fourth order anisotropy is found. The multisteps found in CeP represent the first example of successive phase transitions induced by the de Haas–van Alphen change in the conduction electrons.

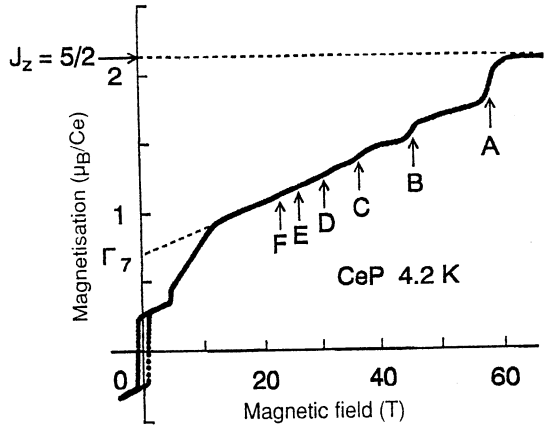

Fig. 8. Multistep magnetisation of CeP. The peaks A to F are Ce-spin steps induced by the de Haas–van Alphen oscillations of conduction electrons.

5. Physics in Highly Correlated Electron Systems

One of the recent research streams in condensed matter physics is the study of highly correlated electron systems where heavy fermions or high T_c superconducting electrons play an important role. High magnetic fields are effective for these electrons because the field destroys their couplings, and elementary processes or couplings can be separated by applying a field. A schematic picture is given in Fig. 9, where the gap structure or dense Fermi level states produced by their correlations are destroyed by applying magnetic fields. Two examples are discussed below.

Much work has been done on the heavy Fermi materials which often reveals the metamagnetic nature. URu_2Si_2 is such a material with a clear three-step

metamagnetism around 30 T (de Visser *et al.* 1987). The observed data are well explained by a model in which the heavy Fermi state in the low field region is destroyed by applying a strong magnetic field, and the exchange interactions between the field-induced magnetic moments on the uranium atoms produce successive metamagnetic transitions (Sugiyama *et al.* 1990). The localised magnetic moment on the uranium atom at zero magnetic field is only $0{\cdot}03\ \mu_B$, reflecting the fact that the f-electrons are not on the uranium site but form a heavy fermion band with the conduction electrons. Under a strong magnetic field, however, the Zeeman energy of the f-electron exceeds the heavy electron coupling energy and a phase transition to the magnetic state occurs. It should be noted that there is a frustrated exchange coupling between the field-induced moments, which gives rise to three metamagnetic steps with normalised net moments $\frac{1}{3}$, $\frac{3}{5}$ and 1 (ferromagnetic), at their corresponding critical fields respectively. The observed data (thick curve) and the three theoretical steps are shown in the upper part of Fig. 10. The heavy Fermi energy and three exchange coupling parameters are determined by the standard mean field approximation. It is emphasised that the present treatment is applicable only when the spin system can be regarded as an Ising network, where a sharp transition is expected.

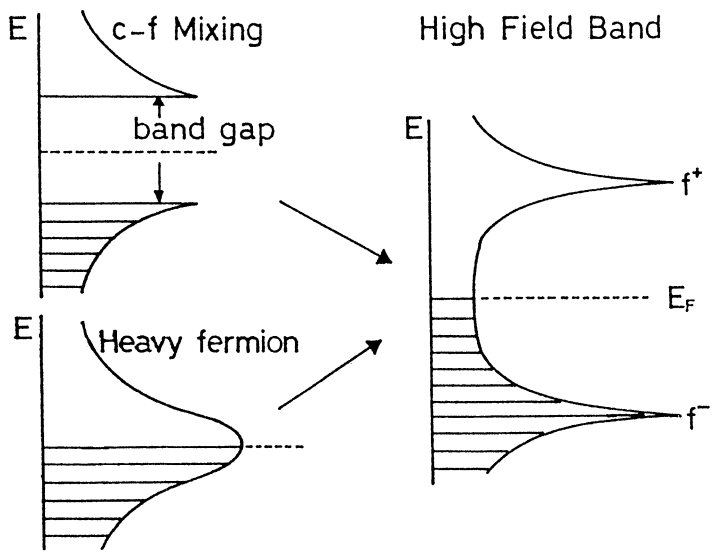

Fig. 9. The c–f mixed density of states (left) are modified by applying a high field (right) where the f-bands are separated from the normal conduction band.

Quenching of the electronic bandgap by a magnetic field is usually difficult even when fields up to 100 T are used. An exceptional result however has been found in YbB_{12} which has a gap of about 100 K above the Fermi level. The origin of the gap is believed to come from the hybridisation of the f and conduction bands. The electrical resistivity is measured under the field up to 50 T and a large negative magnetoresistance is found as is shown in the lower part of

Fig. 10. The resistivity is too small to measure and the compound is substantially metallic around 50 T (Sugiyama *et al.* 1988). This result is explained well by the quenching of the hybridised band due to the magnetic field. The Zeeman energy of the f-electrons plays an important role in this phenomenon. This model is supported by the high field magnetisation experiment where a clear increase in the magnetic moment appears above 50 T. A similar effect is expected for SmB_6, a typical semiconductor with a bandgap due to hybridisation, but the observed magnetoresistance is about one-tenth of that in YbB_{12}. The difference is due to the magnitude of the g-values in both materials.

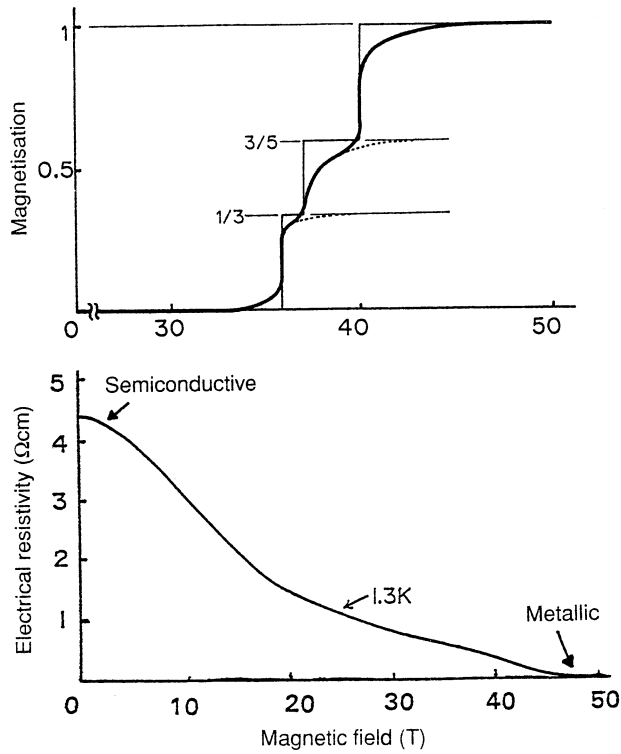

Fig. 10. Three-step magnetisation in URu_2Si_2 (above). The thin lines show the theoretical expectation. The negative magnetoresistance in YbB_{12} which is perfectly metalic above 50 T is shown below.

Another example is the high field effect in high T_c superconductors. Much work on the determination of the upper critical field H_{c2} of the high T_c oxide superconductors has been reported since their discovery in 1986. In these experiments, however, the complete profile of the magnetoresistance curves has been obtained only by our group (Tajima *et al.* 1988), because the H_{c2} values of these materials at low temperatures are much higher than the limit of the usual superconducting magnets. It is emphasised that a complete picture of the

magnetoresistance in all 123 compounds can be obtained even at 4·2 K when a field up to 60 T is applied. For this work, high quality single crystals were grown by an NTT research group (Katsui *et al.* 1987). The thickness of the crystals was about 0·02 mm which is thin enough to avoid eddy current effects and hysteresis.

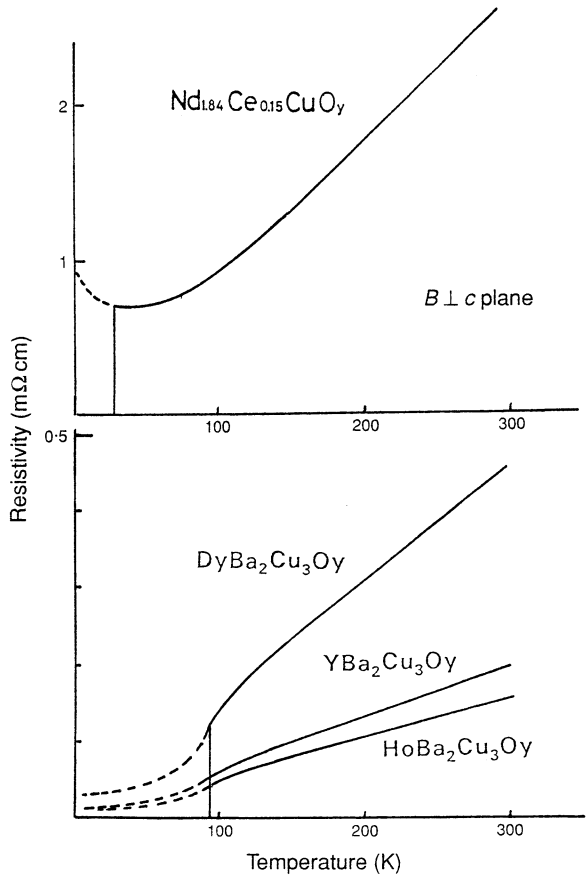

Fig. 11. The log T dependence of the resistivity in an oxide superconductor is shown above. The broken curve is found for high fields. The electrical resistivity of three 123 compounds is shown below. The broken curves are obtained around 50 T.

When the magnetic field is strong enough to break up the superconducting state, one can determine the temperature dependence of the normal electrical resistivity for these compounds. The result is given in the lower part of Fig. 11 (Hikita *et al.* 1989). The full curves are the results of the usual measurements, while the broken curves below T_c are obtained by extrapolating the high field magnetoresistance curves to zero field. The resistivity curves show that the 123 compounds are rather similar to normal metals, which shows a constant resistivity due to impurities at low temperature.

Recently, a single crystal of the high T_c superconductor $Nd_{2-x}Ce_xCuO_y$ has been studied in a field up to 2 T. The superconducting state is completely broken and normal electrical resistivity is obtained at all temperatures, as shown in the upper part of Fig. 11. The temperature dependence of the normal resistivity down to 1·3 K shows a clear resistance minimum. The result can be understood in terms of the two-dimensional weak localisation model (Hidaka *et al.* 1991), so this material is regarded as an intrinsic two-dimensional conduction system.

It is clear that the resistivity minimum is not observed in 123 compounds where the residual resistivity is small and constant. According to the weak localisation theory, the resistivity increase at low temperature does not occur when the residual resistivity is small. Thus the two-dimensionality of 123 compounds is not discounted.

6. Field-induced Crystallographic Transformations

It is generally difficult to induce crystallographic transformations by applying a magnetic field. An exceptional case is the field-induced martensitic transformation. Systematic studies of various alloys have been done by the Shimizu group in Osaka. A striking effect is found in Fe–Ni alloys where the martensitic transformation temperature increases by more than 80 K in a 40 T field (Kakeshita *et al.* 1983).

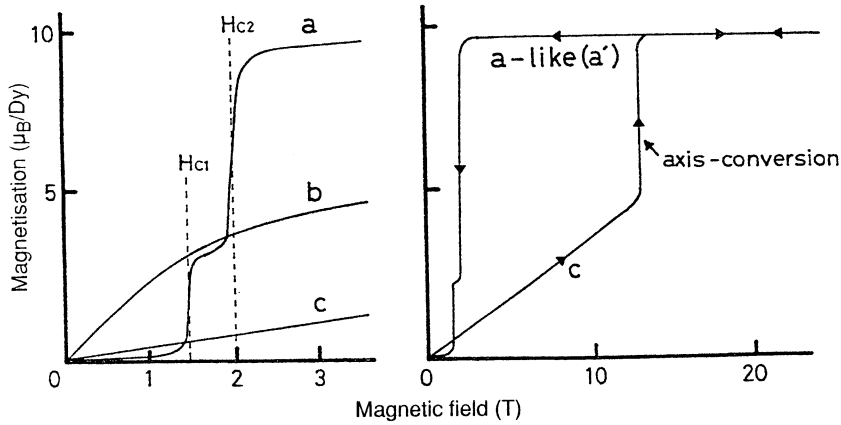

Fig. 12. Metamagnetic transition and Ising axis switching in $DyCu_2$ at 4·2 K.

Another interesting crystallographic modification is observed in $DyCu_2$ (Hashimoto *et al.* 1994), which is an intermetallic rare earth compound with orthorhombic $CeCu_2$ type crystal structure. The Neel temperature is 31·5 K and the Dy spin has an Ising-like axis along the *a*-direction, with a two-step metamagnetism at low fields, as shown to the left of Fig. 12. The gJ value along the *a*-axis is about 10, in accord with the usual Ising-like Dy^{3+} spin. The measured magnetisations along the *b*- and *c*-axes are smooth and small in low fields, as shown in Fig. 12.

In high magnetic fields, however, this material shows the peculiar behaviour given on the right of Fig. 12. The *c*-axis magnetisation is as expected up to

13 T but a sudden jump in magnetisation occurs around 13 T with the same amount of saturation moment along the a-axis. The magnetisation curve under the decreasing field is different from that of the c-axis but very close to the a-axis magnetisation which is labelled a-like(a') in Fig. 12. After this magnetic cycle, the low field magnetisation up to 3 T shows the exchange of the a- and c-axes behaviour, but no change is found along the b-axis. A recovery to the original state is obtained either by warming the crystal above about 100 K or by applying a field higher than 5 T along the a-axis. The c'-axis, which is the original a-axis, shows a weak magnetisation up to 5 T where a sharp step magnetisation appears. In a subsequent decreasing field, a typical a-axis magnetisation is recovered reflecting the switch-back to the original state.

The observed switching of the magnetic axis can be explained by a first order transition model similar to that for the field-induced martensitic transition.

7. Atoms and Molecules in a High Magnetic Field

A high magnetic field is effective for understanding the extensive properties of atoms and molecules. Conventional research is to observe the linear and nonlinear Zeeman effect using various electromagnetic waves.

A unique finding is the field-induced transparency in liquid oxygen (Uyeda *et al.* 1988). The ground state is expressed as $^3\sum_g$. The boiling point of oxygen liquid is 90 K below which the liquid has a blue colour. In a magnetic field, however, we find that the blue colour is quenched and the oxygen becomes transparent. The field-induced transparency is nicely explained in the following way: the blue colour comes from the two-molecule absorption of light with net spin moment zero. Under a high magnetic field, however, all spin moments are parallel so that the light absorption becomes forbidden and the liquid becomes transparent. This is the only example of a field-induced colour change in condensed matter known at present, except the virtual colour change of liquid crystals due to reflection.

The second example discussed in this section is diamagnetic orientation of organic molecules under a magnetic field. Unlike superconductors, diamagnetism of molecules is generally weak and no important physical or chemical problems have been reported. In high magnetic fields, however, the diamagnetic energy is non-negligible and various new phenomena are currently being investigated. One is the diamagnetic Curie–Weiss law found in organic liquids and another is the dimagnetic alignment of biological materials related to human blood. Consider a benzene molecule in a magnetic field. As the diamagnetic shielding current flows in the benzene ring, a field-induced diamagnetic moment appears in the molecule. The magnitude is a maximum when the field is perpendicular to the ring plane. Therefore, the field energy is maximum in this case. Accordingly, the ring is stable when the plane is parallel to the field. The magnitude of the anisotropy energy is, however, very small and only one molecule per 10^6 molecules aligns in this manner at room temperatures under a field of 100 T. The alignment effect can be detected by observing the Cotton–Mouton effect in liquids. The effect is measured by looking at the rotation angle of the incident light polarisation plane under the field, and the angle is proportional to the diamagnetic anisotropy χ_a of molecules. At the beginning of this century, Langevin (1910) pointed out that χ_a is inversely proportional to temperature T. At that time, however, the magnetic fields available were not strong and so they did not see higher order effects. As

the Cotton–Mouton effect is proportional to B^2, high magnetic fields are very effective, and so a series of measurements has been done in Osaka for many organic liquids (Yamagishi *et al.* 1984). The results show that χ_a is proportional to $1/(T-\Theta)$, which is formally similar to the paramagnetic Curie–Weiss law. So, we call this the diamagnetic Curie–Weiss law and the Curie–Weiss constant Θ has been measured for many liquids. Theoretical work has also been done and now it is clear that Θ is due to intermolecular interactions. It is almost zero in benzene but is 165 K for nitrobenzene. This means that intermolecular interaction in nitrobenzene is much stronger than that in benzene. Such interactions are termed 'quadrupolar interactions' in liquids.

When diamagnetic anisotropic molecules are connected and aligned with their anisotropy axes in a definite direction, the net anisotropy increases with increasing molecular number. There are several examples especially among biological materials. The first clear example was found at Grenoble using fibrin, an organic macromolecule in human blood which gives rise to blood clotting. A clear example of magnetically induced alignment taken in Osaka can be seen in Fig. 13. A more recent example is that of alignment in human blood red cells. The diamagnetic alignment occurs in relatively low fields of 1–2 T, which means that a connected molecule consists of more than 10^7 of the unit molecule (Yamagishi *et al.* 1989). The details will not be discussed here, but the alignment suggests that the field effect on the human body might not be negligible even in weak fields. The effect on the human body has attracted much attention not only by scientists but also by the medical profession. However, no clear evidence has ever been reported. The diamagnetic alignment effect reported here may therefore be considered as a breakthrough in this problem. The effect of high fields on the human body, magnetobiology, is a new and growing field.

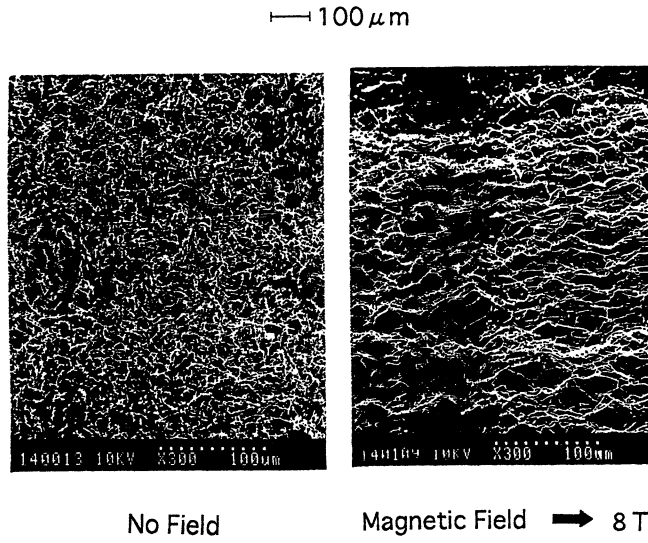

Fig. 13. Diamagnetic orientation of fibrin which is seen to be random in a zero magnetic field (left) while good alignment along the field is seen at right.

8. New Technologies with a High Magnetic Field

A high magnetic field is useful not only in basic science but also in advanced technologies. We show here only one example. We note that the high field facilities can also be used to generate high field gradients dB/dz. A paramagnetic or diamagnetic material feels a force proportional to $B(dB/dz)$. Historically speaking, Faraday constructed a magnetometer using this result, and so it is now

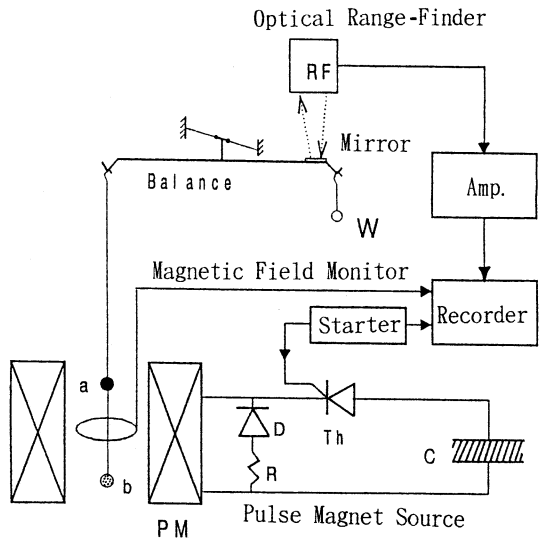

Fig. 14. Block diagram of the dynamic Faraday method. A specimen is set at a and a counter-balance material at b.

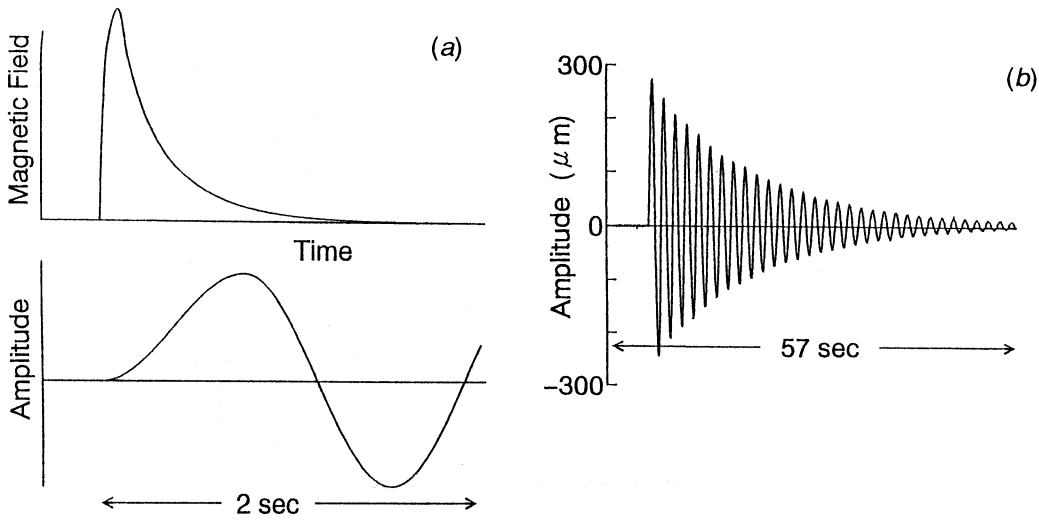

Fig. 15. (*a*) Pulse field profile and the balance oscillation and (*b*) the long-term oscillation profile.

called the Faraday method. In pulsed field facilities, the value of $B(\mathrm{d}B/\mathrm{d}z)$ is about 10^4 times larger than the magnitude in a normal Faraday magnetometer. We have constructed a magnetometer as shown in Fig. 14 for pulsed field work; the method is called the dynamical Faraday method (Date 1994). After one 'pulse field shot', a paramagnetic or diamagnetic specimen on one arm of the balance is acted upon by a force $B(\mathrm{d}B/\mathrm{d}z)$ and so begins to oscillate. An example is shown in Fig. 15 where thin hair of 1·92 mg (diamagnetic) is placed on the balance. The magnetic susceptibility of the specimen can be measured by observing the oscillation and the sensitivity is about 10^3 times higher than that of a SQUID magnetometer. We are now measuring slight changes in biological materials after a light flash or physiological shock. This is only one example and we expect a big future for this new technique.

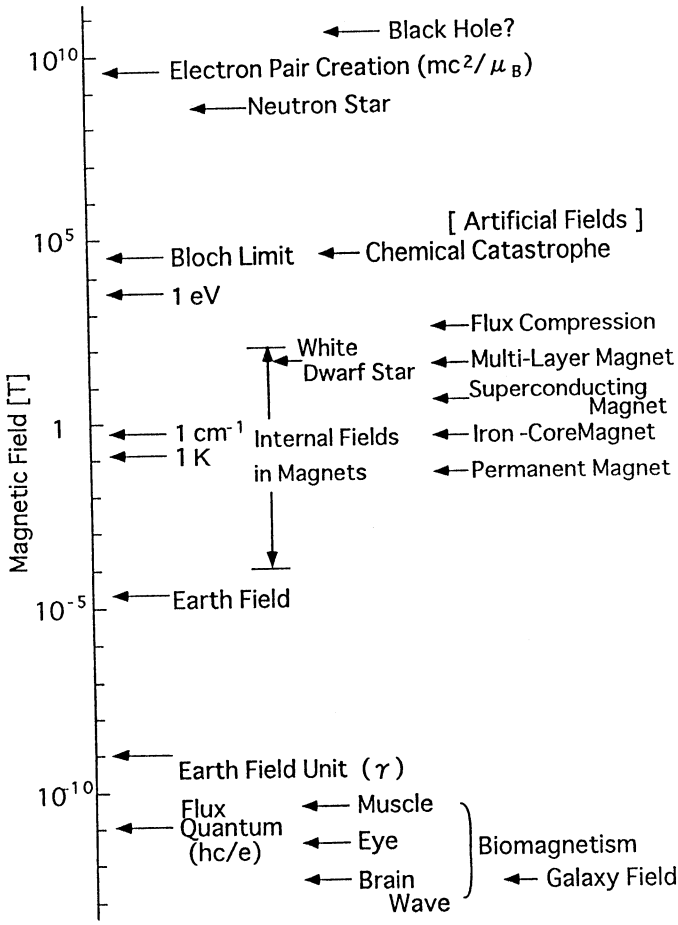

Fig. 16. Natural and artificial magnetic fields.

9. High Fields in the Future

For some time now we have been at the frontier in high magnetic fields and associated technologies. It is difficult to forecast the future, but it may be

valuable to take a 'birds-eye view' of the whole area of high magnetic fields. Various natural and artificially generated magnetic fields, and their corresponding physical phenomena, can be seen in Fig. 16 which employs a logarithmic scale. Useful energy units for one electron spin Zeeman energy are given on the left. For example, it is convenient to remember that (i) 1 T is comparable with 1 K and 1 cm^{-1} and (ii) a quantum magnetic flux (h/e) for an area of 1 cm^2 requires a field of 10^{-10} T. This is the lowest flux density which can be measured using a SQUID. A SQUID can detect a field change of about 10^{-2}–10^{-3} of a quantum flux and this has been used to effect in various biomagnetic studies: the electric current induced magnetic fields associated with brain waves, the eye-field or muscle motions, etc. These represent the lowest fields to be detected at present. By way of comparison, the Earth's magnetic field unit γ (10^{-9} T) is defined as being of the order of Earth field fluctuations, which was the lowest detectable field before the discovery of the SQUID flux. There are also internal magnetic fields in magnetic materials. The highest fields are due to exchange interactions, which are exemplified by ferromagnetic iron and cobalt. In addition, there are magnetic anisotropy fields, dipolar fields and hyperfine fields. These fields are rich in variety and are important research territories. Such fields are also important in magnetic technologies, such as $Nd_2Fe_{14}Bi$ magnetics. In Fig. 16, artificially generated fields are shown on the right. Permanent magnets and iron-core magnets are ~1 T and superconducting magnets can produce ~10–20 T. Our multi-layer magnet can reach 100 T, and flux compression can produce about 500 T, the maximum at present.

On the other hand, natural magnetic fields can vary widely. The Earth's field is of the order of 1 G (10^{-4} T), a standard magnetic unit. The solar field near a black spot is about 0·5 T, the largest field in the solar system. Outside the solar system however, there are very strong magnetic fields. For high density stars, such as a white dwarf, fields of ~100 T can occur. It is believed that these stars have very high densities induced by gravity. Strong magnetic fields are produced by flux compression associated with the collapse. The next stage is gravitational collapse to that of a neutron sea where electrons are captured by protons forming neutrons. In neutron stars where the flux compression is believed to be huge, fields of the order of 10^9 T can be produced.

The magnetic fields we can achieve in the laboratory are thus very low at present. But progress in the generation of magnetic fields in the last two centuries is linear on a logarithmic scale: the maximum field at the end of the 18th century was 10^{-2} T and rising to 1 T at the end of the 19th century. Now, at the end of the 20th century, it is effectively around 100 T. Being optimistic therefore, it could be 10^4 T at the end of the 21st century. If indeed this comes to pass, high field science would see an innovative new world because such fields can affect the chemical bonds in atoms and molecules. Here the spin Zeeman energy is comparable to the chemical binding energy, and so all atoms and molecules will become unstable because the spin-paired bonding state will no longer be stable. We have no information on what materials and phases are possible under this scenario. Another interesting region is at the Bloch limit, while the first Landau level orbit has an area equal to that of the crystallographic unit cell. Hofstadter (1976) has predicted that electronic band structure is reduced in such fields and has drawn the band structure shown in Fig. 17. While the field-induced

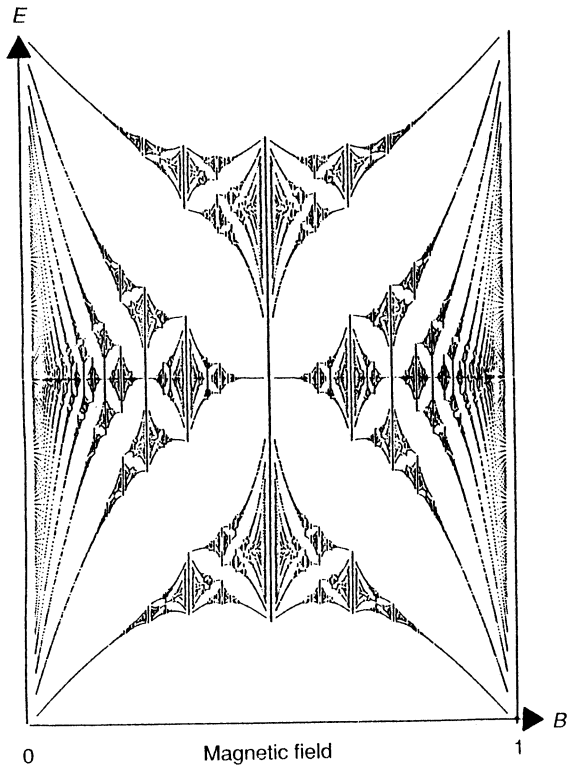

Fig. 17. Band structure of a simple cubic metal under a magnetic field B given by Hofstadter (1976). The field B is normalised to unity when the Landau orbit and a face of the unit cell have the same area.

band reduction is one of the interesting effects at high field, there will also be a big change in atomic and molecular hydrogen. The shape of the hydrogen atom in the ground state is spherical but in high fields it will adopt a prolate shape along the magnetic field. Further, on a neutron star, the shape will be needle-like, due to strong squeezing by the magnetic field. Also a hydrogen molecule in the chemical catastrophe region would have the triplet ground state because the singlet state is not stable. Such ideas will provide further advances in high magnetic field technology.

References

Bitter, F. (1939). *Rev. Sci. Instr.* **10**, 373.
Cnare, E. C. (1966). *J. Appl. Phys.* **37**, 3812.
Date, M. (1975). *J. Phys. Soc. Jpn* **39**, 892.
Date, M. (1976). *IEEE Trans. Mag.* **12**, 1024.
Date, M. (1989*a*). *Physica* B **155**, 119.
Date, M. (1989*b*). 'High Field Magnetism', p. 117 (North Holland: Amsterdam).
Date, M. (1990*a*). *Physica* B **164**, 108.

Date, M. (1990*b*). *J. Magn. Magn. Mater.* **90–1**, 1.
Date, M. (1992). *J. Magn. Magn. Mater.* **104–7**, 2105.
Date, M. (1994). *Physica* B **201**, 1.
Date, M., and Kindo, K. (1990). *Phys. Rev. Lett.* **65**, 1659.
Date, M., and Motokawa, M. (1966). *Phys. Rev. Lett.* **16**, 1111.
Date, M., Motokawa, M., Okuda, K., Hori, H., Mollymoto, H., and Sakakibara, T. (1980). *J. Magn. Magn. Mater.* **15–18**, 1559.
Date, M., Motokawa, M., Yamagishi, A., Hori, H., Sakakibara, T., and Sugiyama, K. (1983*a*). *J. Magn. Magn. Mater.* **31–4**, 140.
Date, M., Sakakibara, T., and Sugiyama, K. (1983*b*). 'High Field Magnetism', p. 41 (North Holland: Amsterdam).
Date, M., Yamagishi, A., Yosida, T., Sugiyama, K., and Kijima, S. (1986). *J. Magn. Magn. Mater.* **54–7**, 627.
Date, M., Yamagishi, A., Hori, H., and Sugiyama, K. (1993). *J. Appl. Phys. Series* **8**, 195.
de Visser, A., de Boer, F. R., Menovsky, A. A., and Franse, J. J. M. (1987). *Solid State Commun.* **64**, 527.
Ewing, J. A., and Low, W. (1889). *Phil. Trans. R. Soc. London*, A **180**, 221.
Fowler, C. M., Garn, W. B., and Caird, R. S. (1960). *J. Appl. Phys.* **31**, 588.
Haseda, T., Wada, N., Hata, M., and Amaya, K. (1981). *Physica* B **108**, 841.
Hashimoto, Y., Kindo, K., Takeuchi, T., Senda, K., and Date, M. (1994). *Phys. Rev. Lett.* **72**, 1922.
Hidaka, Y., Tajima, Y., Sugiyama, K., Tomiyama, F., Yamagishi, A., Date, M., and Hikita, M. (1991). *J. Phys. Soc. Jpn* **60**, 1185.
Hikita, M., Tajima, Y., Fuke, H., Sugiyama, K., Date, M., and Yamagishi, A. (1989). *J. Phys. Soc. Jpn* **58**, 2248.
Hofstadter, D. R. (1976). *Phys. Rev.* B **14**, 2239.
Kakeshita, T., Shimizu, K., Sakakibara, T., Funada, S., and Date, M. (1983). *Trans. Japan Inst. Metals* **24**, 748.
Kapitza, P. L. (1924). *Proc. R. Soc. London* A **105**, 691.
Katsui, A., Hidaka, Y., and Ohtuku, H. (1987). *Jpn J. Appl. Phys.* **26**, L1521.
Katsumata, K., Hori, H., Takeuchi, T., Date, M., Yamagishi, A., and Renard, J. P. (1989). *Phys. Rev. Lett.* **63**, 86.
King, A. R., Jaccarino, V., Sakakibara, T., Motokawa, M., and Date, M. (1981). *Phys. Rev. Lett.* **47**, 117.
Kuroda, T., Sugiyama, K., Haga, Y., Suzuki, T., Yamagishi, A., and Date, M. (1993). *Physica* B **186–8**, 396.
Langevin, P. (1910). *Le Radium* **7**, 249.
Miura, N., Goto, T., and Nojiri, H. (1992). Proc. 6th Int. Conf. on Megagauss Field Generation, Albuquerque (Eds M. Cowan and R. B. Spielman), p. 125 (Nova Science).
Morin, D., Rouchy, J., Yonenobu, K., Yamagishi, A., and Date, M. (1989). *J. Magn. Magn. Mater.* **81**, 247.
Motokawa, M., Kuroda, S., and Date, M. (1979). *J. Appl. Phys.* **50**, 7762.
Sugiyama, K., Iga, F., Kasaya, M., Masuya, T., and Date, M. (1988). *J. Phys. Soc. Jpn* **57**, 3946.
Sugiyama, K., Fuke, H., Kindo, K., Shimohata, K., Menovsky, A. A., Mydosh, J., and Date, M. (1990). *J. Phys. Soc. Jpn* **59**, 3331.
Tajima, Y., Hikita, M., Ishii, T., Fuke, H., Sugiyama, K., Date, M., Yamagishi, A., Katsui, A., Hidaka, Y., Iwata, T., and Tsurumi, S. (1988). *Phys. Rev.* B **37**, 7956.
Uyeda, C., Yamagishi, A., and Date, M. (1988). *J. Phys. Soc. Jpn* **57**, 3954.
Yamagishi, A., and Date, M. (1989). *Physica* B **155**, 91.
Yamagishi, A., Nagao, E., and Date, M. (1984). *J. Phys. Soc. Jpn* **53**, 928.
Yamagishi, A., Takeuchi, T., Higashi, T., and Date, M. (1989). *J. Phys. Soc. Jpn* **58**, 2280.
Yamagishi, A., Yonenobu, K., Kondo, O., Morin, P., and Date, M. (1990). *J. Magn. Magn. Mater.* **90–1**, 51.

Manuscript received 16 August, 1994, accepted 9 February 1995